Light Metals 2013 *Edited by: Barry Sadler*
TMS (The Minerals, Metals & Materials Society), 2013

Effects of Minor Sc Addition on the Microstructures and Mechanical Properties of Al-Zn-Mg-Cu Casting Aluminum Alloy

Yang Guangyu[1], Liu Shaojun[1], Jie Wanqi[1]

[1]State Key Laboratory of Solidification Processing, Northwestern Polytechnical University; No.127 Youyi Western Road, Xi'an, 710072, China

Keywords: Al-Zn-Mg-Cu Aluminum alloy; Sc; Microstructure; Mechanical properties.

Abstract

Effects of *x*%(*x*=0.15, 0.30, 0.45) Sc addition on the microstructures and mechanical properties of metal-mold-casting aluminum alloy Al-6.0Zn-2.8Mg-1.9Cu were studied. It was showed that addition of Sc could reduce α(Al) grain size, modify α(Al)+η($MgZn_2$) eutectic of the experimental alloy, and eliminate Al_7Cu_2Fe phase effectively. It was also found that for the heat treatment experimental alloy, addition of minor Sc could make the second phases along α(Al) grain-boundary and η' meta-stable phase inside α(Al) matrix precipitated more dispersedly, and meanwhile it could promote precipitation of η' phase and decrease its size effectively. The addition of *x*% Sc element could improve the room temperature ultimate tensile strength of the experimental alloy, but had little effects on its plasticity. The room temperature UTS of the experimental alloy with the addition of 0.45%Sc could reach to 510MPa, the maximum value, among the three Sc-content alloys. In addition, it was also found that addition of 0.30% Sc would improve the high temperature tensile strength of the experimental alloy more apparently than those with 0.15% and 0.45% Sc.

Introduction

Al-Zn-Mg-Cu (7xxx) high-strength aluminum alloys are widely used in the aerospace industry for its excellent mechanical properties, the current researches on which are mainly focused on the microstructures and properties of the deformed aluminum alloys[1, 2]. But production of the deformed aluminum alloy has higher demands for the facilities and equipment, which has more complex working procedure, longer production cycle, and higher cost comparing with casting method [3]. In fact, as one of the most important metal molding methods, founding has its unique advantages for its excellent forming ability of the complex castings, low cost and production flexibility. Thus developing the Al-Zn-Mg-Cu group casting aluminum alloy has the important practical significance.

However, acting as the casting alloy, Al-Zn-Mg-Cu group aluminum alloy has intrinsic limitations for its poor casting processability, which being mainly because of its higher alloying extent and broader solidification temperature range which might result in larger porosity tendency, hot tearing tendency and segregation tendency in the castings [4]. How to overcome the above problems is the biggest challenge that Al-Zn-Mg-Cu group casting aluminum alloy facing with.

The foundry property of a kind of alloy can be improved in many ways [5], such as developing the new processing method, lower alloying or micro-alloying method, etc. It was showed that the separate or combined addition of element Titanium (Ti), Manganese (Mn), Erbium (Er), Zirconium (Zr) and Scandium (Sc) could refine the grains of α(Al) matrix significantly, inhibited the re-crystallization process, and improve the mechanical properties of the Al-Zn-Mg-Cu (7xxx) group forging aluminum alloy [6]. It was also found that element Sc was one of the most effective modification agents among the above elements for the Al-Zn-Mg-Cu (7xxx) group forging aluminum alloys.

Based on the previous studies on the Al-Zn-Mg-Cu (7xxx) high-strength deformed aluminum alloys, a new composition Al-Zn-Mg-Cu group casting aluminum alloy, Al-6.0Zn-2.8Mg-1.9Cu-0.1Mn-0.16Zr-0.16Ti experimental alloy was designed in this paper. And the aim of the study was to probe effects of minor Scandium (Sc) addition on the microstructures and mechanical properties of the metal-mold-casting experimental aluminum alloy.

Experimental Method

The experimental alloys were melt in an electrical-resistance furnace with pure Al(99.98), pure Zn(99.9), pure Mg(99.9) and Al-50Cu, Al-5Ti, Al-4Zr, Al-10Mn, Al-4Be, Al-2Sc intermediate alloys (mass fraction, %), and the nominal compositions of the four experimental alloys with *x*% (*x*=0.00, 0.15, 0.30, 0.45, mass fraction) Sc addition were listed in Table1.

Table 1 Nominal composition of the experimental alloys (mass fraction, %)

Experimental Alloy	Zn	Mg	Cu	Mn	Zr	Ti	Be	Al	Sc*
S-00	6.00	2.80	1.90	0.10	0.16	0.16	0.08	Bal.	0.00
S-15	6.00	2.80	1.90	0.10	0.16	0.16	0.08	Bal.	0.15
S-30	6.00	2.80	1.90	0.10	0.16	0.16	0.08	Bal.	0.30
S-45	6.00	2.80	1.90	0.10	0.16	0.16	0.08	Bal.	0.45

*pre-furnace addition amount of Sc element

The prepared experimental alloy was poured into an iron test bar mould at pouring temperature 735℃, and the nominal dimension of the metal-mould-casting standard tensile test specimen was Φ 12 × 60mm. The test specimens were solution heat-treated at 459℃ for 16hr., then followed by water quenching, and aged at 120℃ for 24hr. subsequently.

Microstructure observation was conducted in Olympus PM-G3 type optical microscope transmission (OM) instrument or JEOL JSM-5800 type scanning electron microscope (SEM) instrument, and the phase analysis was conducted in Oxford Inca type X-Ray energy dispersive spectroscope (EDS) instrument. The transmission electron microscope (TEM) observation was conducted in Technai 30F type instrument. The X-ray diffraction (XRD) was performed on X'Pert PRo MPD type instrument in the diffraction angle (2θ) range of between 20° and 90°, using Cu Kα (λ=0.154 nm) as radiation source.

The room temperature and high temperature tensile mechanical properties of the experimental alloys were determined in Zwick 150 type universal tensile testing machine with a 150kN maximum load, and the tensile rate was set at 2mm/min.

Results and Analysis

As-cast Microstructures of the Experimental Alloys

As-cast microstructures of the four experimental alloys were listed in Fig.1. It was showed that the as-cast microstructure of Sc-free (S-00) experimental alloy was consisted of flower-like equiaxed grains, and the semi-continuous netted black second phase was distributed along the grain boundary, meanwhile some black dotted second phases existing inside α(Al) grains. From Fig.1 b, c and d, it was showed that α(Al) grains of Sc-content (S-15, S-30 and S-45) experimental alloys got considerable refined to a different degree, among which α(Al) grain size of S-45 experimental alloy was the minimum. The main reason for this was that addition of Sc element to the melt of the experimental alloys resulted in the formation of large quantity of crystal nucleus of Al_3Sc, $Al_3(Zr, Sc)$ or $Al_3(Ti, Sc)$ [7], which would promote heterogeneous nucleation of α(Al) matrix during the solidification of the Sc-content experimental alloys, and thereupon they got fine grain structure. However, it was found that there was an optimum adding amount of Sc for a certain kind of the aluminum alloy [8], and thus the refining effect had differences for Sc-content (S-15, S-30, S-45) experimental alloys, as showed in Fig.1 b, c and d.

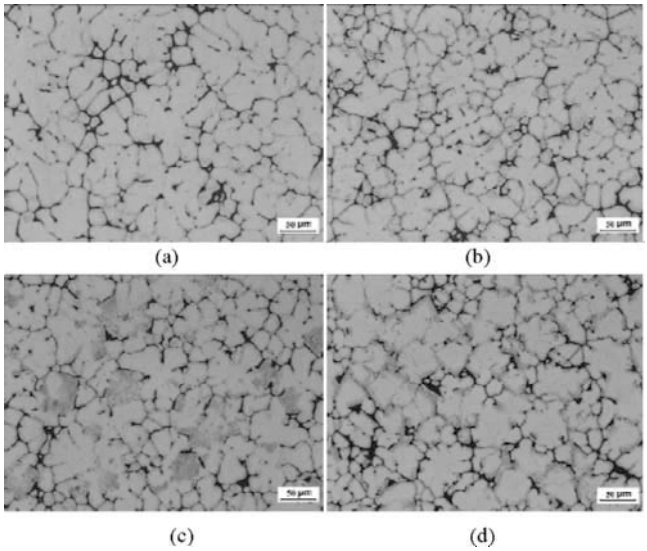

Fig.1 Microstructures of the as-cast experimental alloys
(a) S-00, (b) S-15, (c)S-30, (d)S-45

The high magnification microstructures of the four experimental alloys were listed in Fig. 2. From Fig.2a, it was watched that there was a kind of gray thin particle phase inside α(Al) matrix which size being nearly 2~6μm, as shown by the arrow in Fig2a. The EDS analysis results of the gray thin particle phase were given in Fig.3. It was found that the chemical composition of this phase was close to Al_7Cu_2Fe, and according to literature [3, 9], it was deduced as Al_7Cu_2Fe phase. It was worth pointing that Al_7Cu_2Fe phase did not occur in the microstructures of the Sc-content (S-15, S-30, S-45) experimental alloys, as listed in Fig.2b, c, and d. Being a high chemical activity rare earth element, Sc element had a strong affinity for iron (Fe) and hydrogen (H_2) in the aluminum alloy melt and could form the associated compounds, by which it could remove the inclusion in the melt or modified the morphology of the inclusion [10]. The disappearance of Al_7Cu_2Fe phase in the Sc-content experimental alloys may be the results of Sc element reacting with Al_7Cu_2Fe phase and forming another heavier compound which would precipitate to the bottom of the crucible.

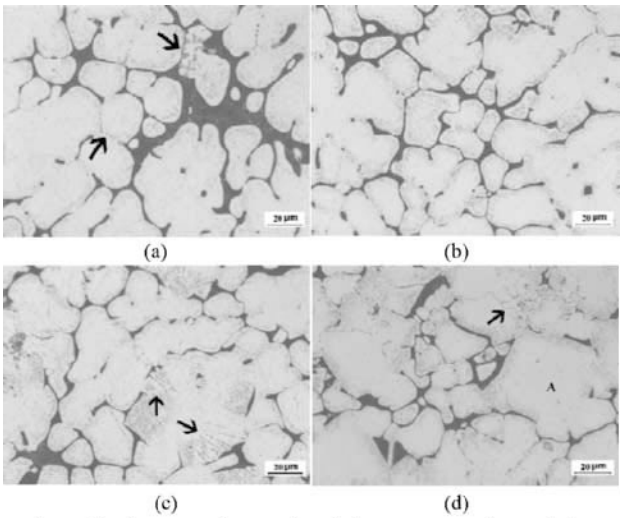

Fig.2 High times OM photographs of the as-cast experimental alloys
(a) S-00, (b) S-15, (c) S-30, (d) S-45

It also could be seen that α(Al) grain of Sc-free (S-00) experimental alloy was round and smooth, with some little black dotted phases existing inside it. When the Sc addition amount being 0.15%, the roundness of α(Al) grain got deviated, and the quantities of little black dotted phases inside α(Al) grain got somewhat increased. And when the Sc addition amount increasing to 0.30%, the roundness of α(Al) grain got further deviated, and the little black dotted phases inside α(Al) grain was distributed as spokes-like, as shown by the arrow in Fig2c. When the Sc addition amount being up to 0.45%, α(Al) grain boundary had a trend of straightening, and even occurred as triangular-like or rectangular-like appearance. Meanwhile, the little black dotted phases inside α(Al) grain was distributed as bending-line-like, as shown by the arrow in Fig2d.

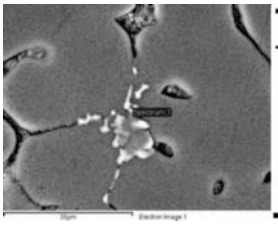

Element	Atomic fraction, %
Mg	2.72
Al	75.61
Mn	3.14
Fe	4.60
Cu	13.92

Fig.3 BSE image and EDS analysis results of gray second-phase in the as-cast S-00 alloy

The SEM morphologies of the eutectics in the four as-cast experimental alloys were listed in Fig.4. It was showed that the eutectic lamellae of S-00 experimental alloy were stubby, just presenting wormlike structure; and that of S-15 experimental alloy were fine and closely woven, presenting short-crumb-like structure; and the eutectic lamellae of S-30 experimental alloy was strip-like, presenting clearly well arranged structure, which eutectic spacing was larger than that of S-15 experimental alloy, and close to that of S-00 experimental alloy. Meanwhile, the

eutectic lamellae of S-45 experimental alloy were fine fleece-like, and its eutectic spacing was the finest among them.

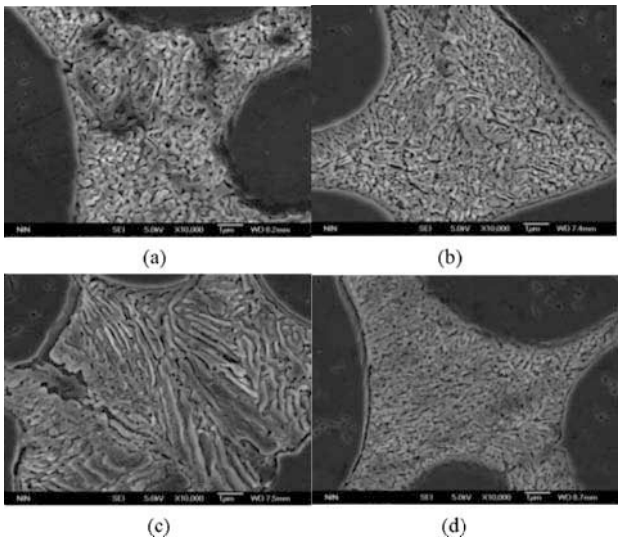

Fig.4 The SEM morphologies of the eutectics in the as-cast experimental alloys
(a) S-00, (b) S-15, (c) S-30, (d) S-45

The XRD patterns of the as-cast S-00 and S-30 experimental alloy were presented in Fig.5 respectively. And the DSC analysis results of both experimental alloys were also given in Fig.6. From them, it was easy to found that the as-cast microstructure of these two alloys were both mainly consisted of α(Al) matrix and α(Al)+η($MgZn_2$) eutectic, and that Sc addition did not alter the main phase make-up of S-00 experimental alloy.

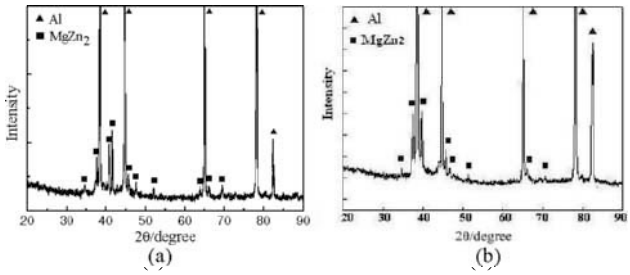

Fig.5 XRD patterns of the as-cast S-00 and S-30 experimental alloy
(a) S-00, (b) S-30

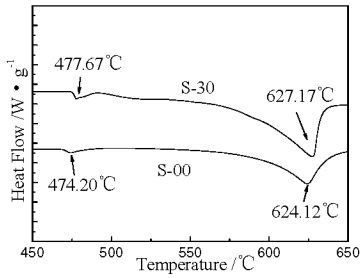

Fig.6 DSC patterns of as-cast S-00 and S-30 experimental alloy

It was also proved that S-15 and S-45 experimental alloy had the same main phase make-up as that of S-30 experimental alloy.

The further observation on as-cast microstructure of the four experimental alloys revealed that there existed some bright white globular or short-stick-like phase in the middle or edge of the eutectic, as shown in Fig.7a. And the EDS analysis results of this kind of phase in S-00 experimental alloy were also presented in Fig.7b. It was found that the composition of the bright white phase was close to that of T($Mg_3Zn_3Al_2$) phase. The TEM–BF morphology of the bright white phase in S-00 experimental alloy was also showed in Fig.7c and composite electron diffraction pattern (EDP) of α(Al) and bright white phase shown by the circle in Fig.7c was given in Fig.7d. It was determined that this kind of bright white phase was T($Mg_3Zn_3Al_2$) phase, which lattice parameter a=0.1415 nm with tI162 type crystal structure, which orientation relationship with α(Al) matrix was $[001]_{Al}//[111]_T$.

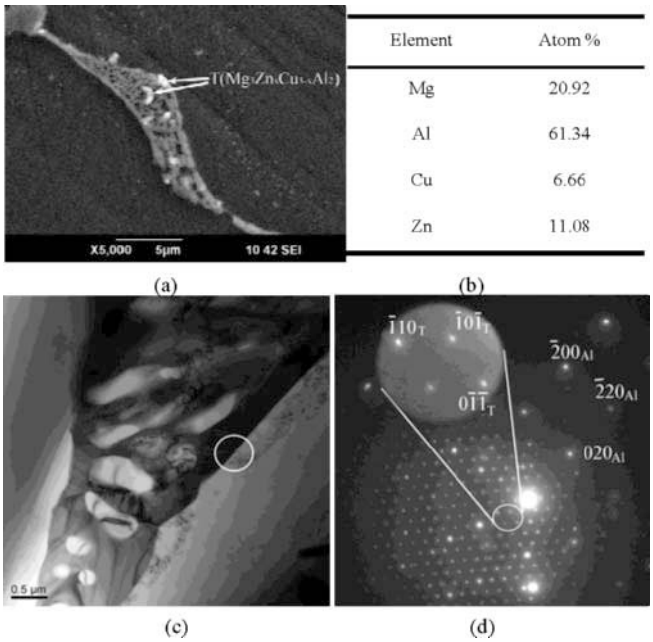

Fig.7 SEM morphology (a) and EDS analysis results (b) of the bright white second phase, TEM-BF morphology of α(Al)+η($MgZn_2$) eutectic (c) and composite EDP of Al and bright white phase T shown by the circle in Fig.7c (d) in S-00 experimental as-cast alloy

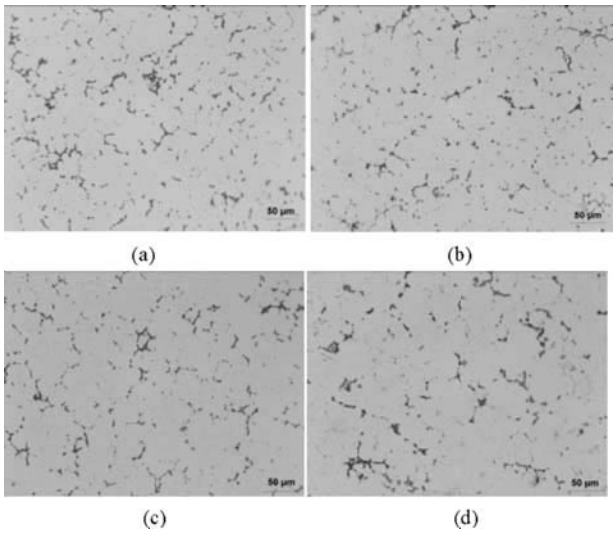

Fig.8 OM morphology of the four quenched experimental alloys after aging (120℃, 24h) (a) S-00, (b) S-15, (c) S-30, (d) S-45

It was worth noting that there was 6.66% Cu dissolved in T ($Mg_3Zn_3Al_2$) phase from EDS analysis results shown in Fig.7b,

which substituted for part of Zn atoms in T($Mg_3Zn_3Al_2$) phase because of the atomic radius of Cu (r_{Cu}=12.8nm) being similar to that of Zn (r_{Zn}=13.9nm). Combined with literature [11], the molecular formula of T($Mg_3Zn_3Al_2$) phase was adapted to T ($Mg_3Zn_xCu_{3-x}Al_2$).

It came to the same conclusion that the bright white globular or short-stick-like phase in the Sc-content experimental alloys was also determined to be T($Mg_3Zn_xCu_{3-x}Al_2$) phase and the related images and analysis about them were omitted here.

Heat-treatment Microstructures and the Mechanical Properties of the Experimental Alloys

OM morphologies of the four quenched experimental alloys after aging treatment were showed in Fig.8. It was found that the second phases along α(Al) grain-boundary in Sc-content experimental alloy precipitated more dispersedly than Sc-free experimental alloy.

The inter-granular second phase in S-00 experimental alloy was determined as shown in Fig.9. It was concluded that the heat-treatment microstructures of S-00 experimental alloy were mainly consisted of α(Al) matrix, α(Al)+η($MgZn_2$) eutectic, some S(Al_2CuMg) phase and Al_7Cu_2Fe phase. It was worth noting that S(Al_2CuMg) phase appeared in the heat-treatment microstructures of S-00 experimental alloy, instead of T($Mg_3Zn_xCu_{3-x}Al_2$) phase, which appeared as gray-white-like and being formed during the solid solution treatment process of S-00 experimental alloy. And this has been confirmed by the literature [3, 9, 12].

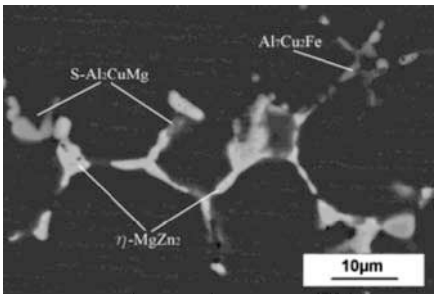

Fig.9 high magnified SEM images of the quenched S-00 experimental alloy after aging (120℃, 24h)

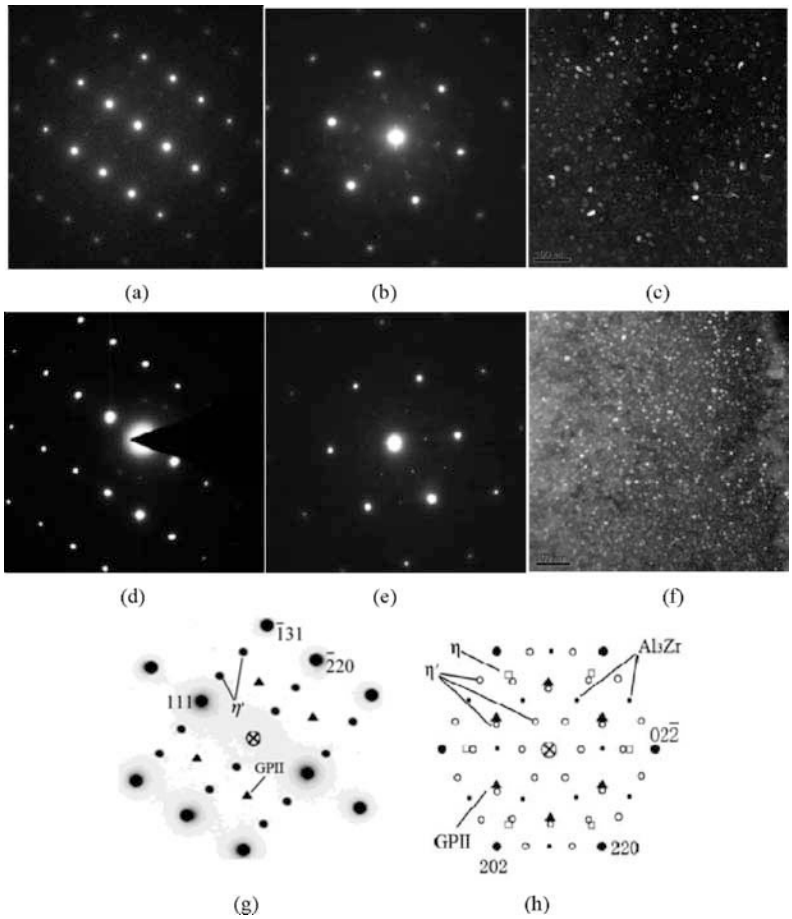

Fig.10 The analysis on the precipitates within α(Al) matrix of quenching S-00 experimental alloy after aging (a), (b), (c) and that of quenching S-30 experimental alloy after aging (d), (e), (f)
(a) and (d) SAEDPs in $<112>_{Al}$ projection direction, (b) and (e) SAEDPs in $<111>_{Al}$ projection direction, (c) and (f) dark field images of precipitates were taken from η′ spots located at $2/3\{220\}_{Al}$ positions of <112> zone axis, (g) and (h) schematic representation in $<112>_{Al}$ and $<111>_{Al}$ projection direction, respectively.

It was also confirmed that the microstructure of Sc-contained (S-15, S-30, S-45) experimental alloy was also mainly consisted of α(Al) matrix, α(Al)+η($MgZn_2$) eutectic and some S(Al_2CuMg) phase, but except for Al_7Cu_2Fe phase.

The selected area electron diffraction patterns (SAEDPs) of the precipitates within α(Al) matrix of S-00 and S-30 heat treatment experimental alloy, TEM dark field image of precipitation phases inside α(Al) matrix, and schematic representation of the projection direction $<112>_{Al}$ and $<111>_{Al}$ were listed in Fig.10. It was found that there existed GPII zone and η' meta-stable phase within α(Al) matrix of these two experimental alloys. From Fig.10c, it was found that η' meta-stable phase within α(Al) matrix in S-00 experimental alloy presented a globular or ellipsoidal appearance, which diameter range being 1.2~32.7nm and distribution density of η′ phase being of about $1.6\times10^{16}m^{-2}$. From Fig.10c, it was concluded that η' meta-stable phase inside α(Al) matrix in S-30 experimental alloy presented a more uniform distributed globular or ellipsoidal appearance, which diameter range being 1.0~20.0nm and distribution density of η′ phase being of about $2.5\times10^{16}m^{-2}$. Thus we came to the conclusion that Sc element could promote precipitation of η' meta-stable phase and decrease the size of η' phase effectively, and also made η' phase distributed more dispersedly, all of which would strengthen S-30 experimental alloy more effectively. And this would also be further proved by determination of mechanical properties of the four experimental alloys.

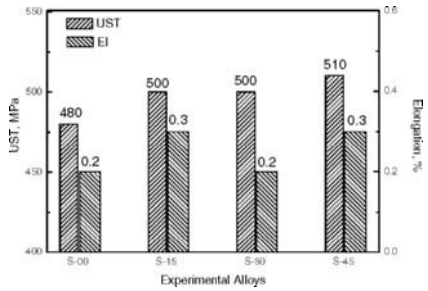

Fig .11Tensile properties of four experimental alloys at room temperature

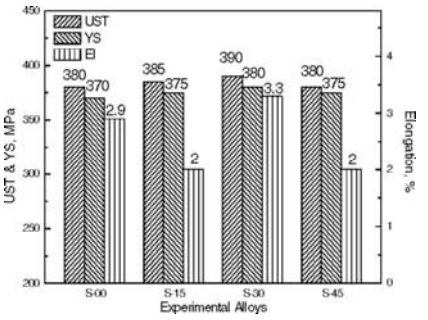

Fig .12 Transient tensile properties of experimental alloys at 200℃

The room mechanical properties of the four experimental alloys were listed in Fig.11, and the high temperature transient mechanical properties of the four experimental alloys were also showed in Fig.12. It was found that addition of Sc could improve the room temperature ultimate tensile strength of the experimental alloy, but had little effects on its plasticity. The room temperature UTS of the experimental alloy with the addition of 0.45%Sc could reach to 510MPa, the maximum value, among the three Sc-content alloys. It was also found that addition of 0.30% Sc would improve the high temperature tensile strength of the experimental alloy more apparently than those with 0.15% and 0.45% Sc.

Conclusions

It was showed that addition of minor Sc could reduce α(Al) grain size, modify α(Al)+η(MgZn2) eutectic of the as-cast experimental alloy, and eliminate Al_7Cu_2Fe phase effectively.

It was also found that for the heat treatment experimental alloy, addition of minor Sc could make the second phases along α(Al) grain-boundary and η' meta-stable phase inside α(Al) matrix precipitated more dispersedly, and meanwhile it could promote precipitation of η' phase and decrease its size effectively.

The addition of *x*% Sc element could improve the room temperature ultimate tensile strength of the experimental alloy, but had little effects on its plasticity. The room temperature UTS of the experimental alloy with the addition of 0.45%Sc could reach to 510MPa, the maximum value, among the three Sc-content alloys. In addition, it was also found that addition of 0.30% Sc would improve the high temperature tensile strength of the experimental alloy more apparently than those with 0.15% and 0.45% Sc.

Reference

1. A. Deschamps,et al., "In situ evaluation of dynamic precipitation during plastic straining of an Al–Zn–Mg–Cu alloy," *Acta materialia*, 60(2012), 1905-1916
2. M. Liu, B. Klobes and K. Maier, "On the age-hardening of an Al–Zn–Mg–Cu alloy: A vacancy perspective," *Scripta Materialia*, 64(2012), 21-24
3. Yang G Y, et al., "Microstructures and room temperature mechanical properties of Al-6.3Zn-2.8Mg-1.8Cu casting Aluminum alloy", *Acta Metallurgica Sinica*, 48(2) (2012), 211-219
4. Tian R Z, Casting aluminum alloy, (Chang Sha, NY: Central South University Press, 2006), 144-150
5. J. Dong, et al., "A new way to cast high-alloyed Al–Zn–Mg–Cu–Zr for super-high strength and toughness", *Journal of Materials Processing Technology*, 171(2006), 399-404
6. H. C. Fang, et al., "Effect of Zr, Cr and Pr additions on microstructures and properties of ultra-high strength Al–Zn–Mg–Cu alloys", *Materials Science and Engineering: A*, 528(2011), 7606-7615
7. O. N. Senkov, et al., "Precipitation of Al3(Sc,Zr) particles in an Al–Zn–Mg–Cu–Sc–Zr alloy during conventional solution heat treatment and its effect on tensile properties", *Acta materialia*, 56(2008), 3723-3738
8. J RΦyset, N Ryum. "Scandium in aluminium alloys", *International Materials Reviews*, 50(1) (2005), 19-44
9. Fan X G., "Study on the microstructures and mechanical properties and the fracture behavior of the Al–Zn–Mg –Cu–Zr alloys" (Ph.D. Thesis, Harbin Institute of Technology, 2007), 30-34
10. BIE S Q, YAO S J, CHEN W, "Effects of Ni on hardness and microstructure of Ultra high strength aluminum alloy Al-Zn-Mg-Cu-RE", *Material and Heat treatment*，35(24) (2006), 31-33.
11. C. Mondal, A. K. Mukhopadhyay, "On the Nature of T($Al_2Mg_3Zn_3$) and S(Al_2CuMg) Phase Present in As-cast and Annealed 7055 Aluminum Alloy", *Materials Science and Engineering A*, 391(2005), 367-376.
12. Fan X G, et al., "Characterization of precipitation microstructure and properties of 7150 aluminium alloy", *Mat Lett*, 60(2006), 1475